Available online at www.sciencedirect.com

ScienceDirect

Procedia Structural Integrity 44 (2023) 536–543

Structural Integrity Procedia

www.elsevier.com/locate/procedia

XIX ANIDIS Conference, Seismic Engineering in Italy

Push ‘o ver: numerical simulation of the Castel di Lama pushover test through a force-based equivalent frame model

Daniela Addessi[a], Domenico Liberatore[b]*, Luigi Sorrentino[b], Allen Dudine[c], Andrea Dall’Asta[d], Michele Morici[d], Antonio Boccamazzo[e], Oreste De Simone[e], Giacomo Buffarini[f], Paolo Clemente[f]

[a] *Department of Structural and Geotechnical Engineering, Sapienza University of Rome, via Eudossiana 18, 00184 Rome*
[b] *Department of Structural and Geotechnical Engineering, Sapienza University of Rome, via Gramsci 53, 00197 Rome*
[c] *Fibre Net S.p.A., Via Jacopo Stellini 3, Z.I.U. 33050 Pavia di Udine, Italy*
[d] *School of Architecture and Design, University of Camerino, viale della Rimembranza 3, 63100 Ascoli*
[e] *EAS Ingegneria Srl, via B. Peruzzi 6, 41012 Carpi (MO)*
[f] *ENEA, Casaccia Research Centre, via Anguillarese 301, 00123 Rome*

Abstract

The experimental pushover test performed on the Castel di Lama building is studied by means of a finite element procedure based on the equivalent frame model with the aim to test the ability of this widespread model to reproduce the experimental results and the collapse mechanisms. Pier and spandrel macroelements are modelled as Timoshenko beams with plastic hinges to take into account shear and bending failures. Assuming the nodes as infinitely rigid and resistant, it is possible to model them by introducing properly sized offsets at the ends of pier and spandrel macroelements. A force-based formulation is adopted for the macroelement, taking advantage of its higher performances in terms of accuracy and efficiency with respect to the classical displacement-based method, and the capability of naturally avoiding shear-locking problems.
The response of the building walls, either unreinforced or reinforced, is analysed in terms of resisting forces, story displacements and damage patterns, and compared with the experimental results.

Keywords: masonry; pushover; plastic hinge; finite element; equivalent frame.

* Corresponding author. Tel.: +39-06-49919155.
E-mail address: domenico.liberatore@uniroma1.it

10.1016/j.prostr.2023.01.070

1. Introduction

In recent decades, several solutions have been developed for the structural reinforcement of masonry buildings which make use of innovative materials, such as Fiber Reinforced Polymers (FRP).

FRP are a wide range of composite materials, consisting of an organic polymeric matrix with which a continuous fiber reinforcement characterized by high mechanical properties is impregnated. The FRP covered in this study is the GFRP (Glass Fiber Reinforced Polymer) mesh. Unlike FRP stripes, the application of a GFRP mesh does not take place using epoxy resins, but through the use of inorganic matrices. This technique is subject of research in order to develop a valid alternative to the technique with epoxy resins, which presents problems of durability, poor compatibility with historical masonry and poor performance at temperatures above 60-80°C.

The purpose of this research project is the assessment of the seismic capacity of an existing masonry building classified as unusable following the 2016-2017 Central Italy earthquake. The building was divided into two parts, almost identical and structurally independent. The first part (building 1) was tested as built, the second (building 2) after being reinforced with GFRP. The two buildings underwent an in-situ pushover test, with the lateral loads applied by means of hydraulic jacks and a steel reaction frame, Boccamazzo et al. (2022), Dudine et al. (2022).

In this paper, the experimental test is simulated by means of the equivalent frame model based on a force-based macroelement, aiming at reproducing forces, displacements and failure mechanisms.

2. Equivalent frame model

The adopted Finite Element (FE) model is based on the macroelement approach and equivalent frame formulation which, despite its simplicity, is very effective in returning the most important results from the technical point of view, Raka et al. (2015), Gatta et al. (2018), Siano et al. (2018), Peruch et al. (2019).

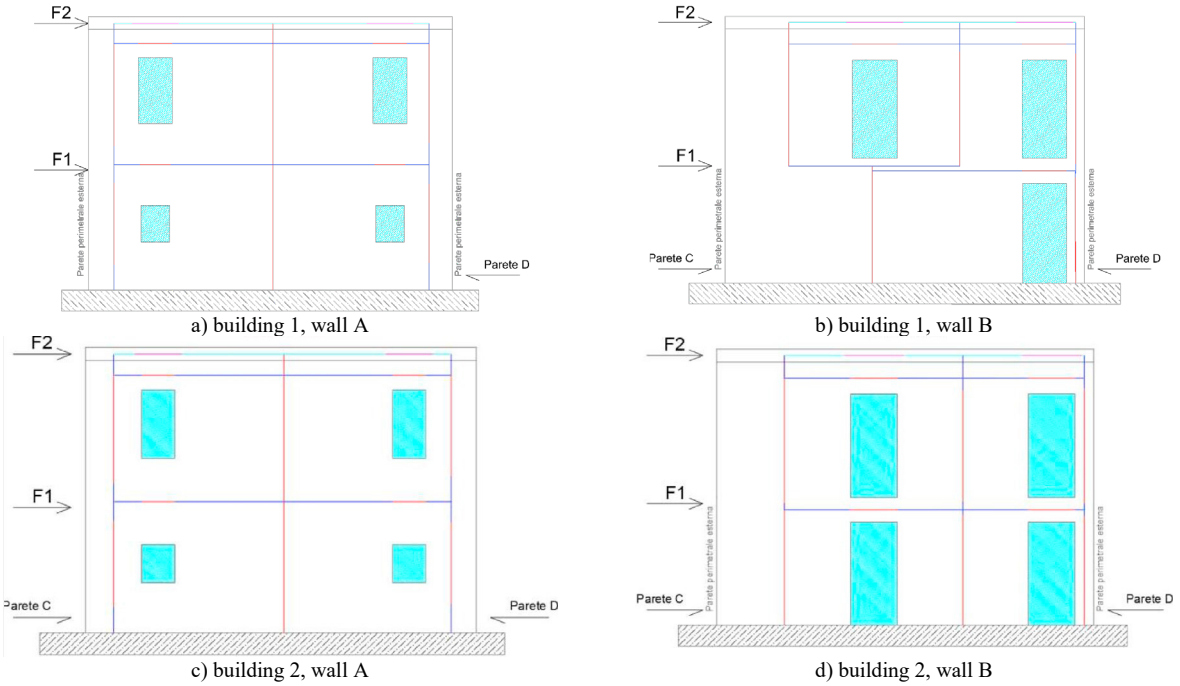

Fig. 1. Equivalent frame models of the walls.

Each wall is schematized by means of a set of pier elements with vertical axis, spandrel elements with horizontal axis and node elements (Fig. 1). Pier and spandrel elements are modelled as Timoshenko beams with plastic hinges to take into account shear and bending failures. Assuming the nodes as infinitely rigid and resistant, it is possible to model them by introducing properly sized offsets at the ends of pier and spandrel elements.

The behavior of pier elements is assumed to be elastic-plastic with displacement limit. The stiffness matrix in the initial elastic phase assumes the usual form for beam elements according to Timoshenko theory. The height of the deformable part, or "effective height", of pier elements is defined according to the formulation of Dolce (1991), to approximately reproduce the deformability of masonry in the node areas.

Spandrel elements are formulated in a similar way, but with some differences. Rigid offsets are maintained, thus defining the effective length of the element. If the openings are vertically aligned, the effective length is assumed to be equal to the free span of the openings, otherwise the effective length is determined as the average of the free spans of the openings above and below the spandrel.

3. Force-based macroelement model

The numerical models of the two buildings are developed by adopting the macroelement approach described in contributions of Addessi et al. (2015), Liberatore and Addessi (2015), Sangirardi et al. (2019).

This relies on a force-based equivalent frame formulation, taking advantage of its higher performances in terms of accuracy and efficiency with respect to the classical displacement-based method, and the capability of naturally avoiding the shear-locking problems. By considering the building main walls, a two-dimensional 2-node Timoshenko beam element is used to model each pier and spandrel, by properly introducing the rigid zone lengths at the intersection between them, as shown in Fig. 2 where the nodal displacement degrees of freedom are also shown. According to the adopted equilibrated formulation, the element state determination is referred to the basic system obtained by eliminating the rigid body modes. The resulting nodal displacements and forces are listed in vectors $\mathbf{q} = [q_1 \;\; q_2 \;\; q_3]^T$ and $\mathbf{Q} = [Q_1 \;\; Q_2 \;\; Q_3]^T$, shown in Fig. 2, where q_1 and q_2 denote the nodal deformational rotations and q_3 is the axial elongation, while Q_1 and Q_2 are the bending moments at the end nodes i and j, and Q_3 is the axial force.

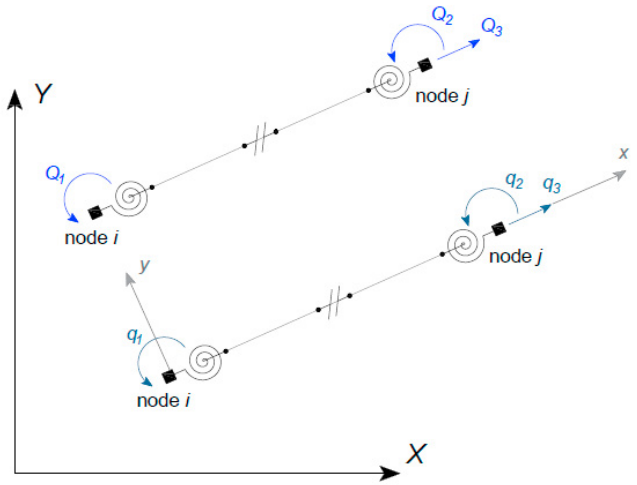

Fig. 2. 2D beam finite element: nodal forces (top) and displacement (bottom) in the element basic reference system.

To describe the nonlinear mechanisms, typically occurring in masonry walls when subjected to in-plane loadings, a lumped hinge approach is considered by introducing two nonlinear flexural hinges located at the beam end nodes and a nonlinear shear link, arranged in series with the central elastic beam, as schematically reported in Fig. 2.

The element tangent stiffness matrix and nodal force vector are derived, in the framework of the force-based approach, by first evaluating the element tangent flexibility matrix and nodal residual displacements. Accounting for

the series arrangement of the nonlinear devices and elastic beam, and considering that nonlinear hinges are introduced only for flexural and shear behavior, while beam axial response is linear elastic, the element tangent flexibility matrix results as follows:

$$F = \begin{bmatrix} \frac{L_e}{3EI} + F_{bi} + \frac{F_S}{L_e^2} & -\frac{L_e}{6EI} + \frac{F_S}{L_e^2} & 0 \\ -\frac{L_e}{6EI} + \frac{F_S}{L_e^2} & \frac{L_e}{3EI} + F_{bj} + \frac{F_S}{L_e^2} & 0 \\ 0 & 0 & \frac{L_e}{EA} \end{bmatrix} \tag{1}$$

where L_e is the length of the element deformable portion, resulting from the presence of rigid end-offsets, EA and EI are the axial and flexural stiffnesses of the beam, and F_{bi}, F_{bj}, F_s are the tangent flexibility contributions of the flexural hinges and shear link.

The element is, then, introduced in a global finite element code based on the classic displacement approach and Newton-Raphson algorithm. Moreover, the nodal residual quantities are determined in terms of the element nodal deformational rotations, then transformed into internal basic forces **Q**.

The constitutive response of the nonlinear hinges follows a classical rigid-plastic law. The flexural and shear strengths are evaluated according to the Italian National Code NTC (2018). The ultimate moment M_u at the end sections of the element, in case of rectangular sections, results:

$$M_u = \frac{1}{2}\sigma_0 \left(1 - \frac{\sigma_0}{0.85\, f_c}\right) l^2 t \tag{2}$$

where l and t are the section sizes, width and thickness, respectively, σ_0 is the mean normal stress acting on the section, and f_c is the masonry compressive strength. The shear strength is defined by the shear-sliding criterion as:

$$V_t = f_v\, l'\, t \tag{3}$$

where l' is the length of the compressed zone of the panel end section and f_v the masonry shear strength, evaluated as:

$$f_v = f_{v0} + 0.4\, \sigma_n \leq f_{vLIM} \tag{4}$$

being f_{v0} the masonry shear strength in the absence of normal stress, and σ_n the mean normal stress on the compressed zone of the cross section, while f_{vLIM} denotes the shear strength limit value. In the case of old masonry, characterized by irregular fabric or weak blocks, the diagonal cracking criterion is adopted and the shear strength evaluated as:

$$V_t = \frac{f_t}{b}\, l\, t \sqrt{1 + \frac{\sigma_0}{f_t}} \tag{5}$$

where f_t is the tensile strength for diagonal cracking and b is defined as:

$$b = \frac{L_e}{l} \qquad 1 \leq b \leq 1.5 \tag{6}$$

To solve the evolution problem of the nonlinear flexural and shear devices, a predictor-corrector procedure is implemented. Thus, at each Newton-Raphson iteration of the global solution procedure, the displacement increments at the end nodes of the element are given, and a predictor element stress field is calculated using the tangent flexibility matrix at the previous iteration. Then, the corrector phase is performed adopting a return algorithm, based on the Haar-Kármán principle, which brings back the stress field onto the bounding surface of the strength domain. The Karush-Kuhn-Tucker conditions, necessary and sufficient for the global minimum in case of convex programming problems, and the gradient projection method are adopted. The described beam FE and solution algorithm were introduced in the FE program FEAP used to perform the nonlinear numerical analyses on the two buildings.

4. Numerical results

Building 1

Building 1 is the portion of the construction that was simply restored, repairing the damage of the 2016-2017 Central Italy earthquake. The mechanical properties adopted for masonry are reported in Table 1.

Table 1. Mechanical properties of masonry (building 1).

f (MPa)	f_{v0} (MPa)	τ_0 (MPa)	f_h (MPa)	E (MPa)	G (MPa)
4.550	0.152	0.076	2.275	1278	549

The pushover curves of walls A and B, calculated through the equivalent frame model, are reported in Fig. 3, assuming the control point at the top of the walls. The pushover curve of wall A has a plastic branch up to a displacement slightly greater than 20 mm, then undergoes a sudden decrease in force, a second plastic branch up to 30 mm, and finally collapses. The pushover curve of wall B has a plastic branch up to the 30 mm displacement and then collapses. The location and type of plastic hinges at collapse are reported in Fig. 4.

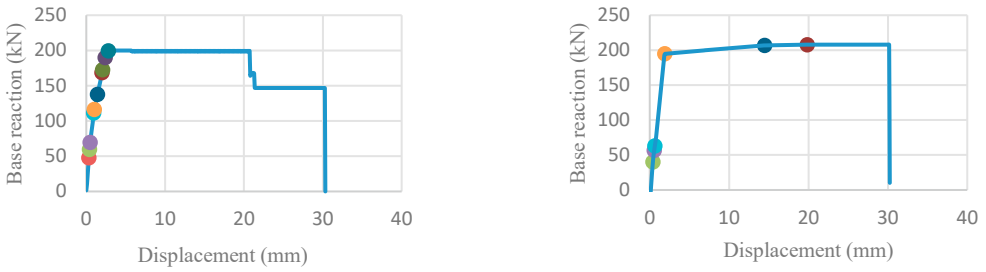

a) wall A b) wall B

Fig. 3. Force-displacement numerical response curves for building 1: colored circles correspond to the hinges depicted in Fig. 4.

a) wall A b) wall B

Fig. 4. Plastic hinge distribution at collapse for building 1: colored symbols indicate hinges corresponding to the circles depicted in Fig. 3 (circle: flexural hinge, parallelogram: shear link).

The comparisons between the numerical pushover curves and the experimental ones are shown in Fig. 5. The control point is assumed either at the first story or at the second story. The diagrams report the sum of the forces of walls A and B as function of their mean displacement, considering that the displacements of the two walls are almost identical. It can be observed that the numerical results are very close to the experimental ones in terms of strength. On the other hand, differences in the type of mechanism can be noted: while the experimental test activates a mechanism at the second story, the numerical analysis envisages a mechanism at the first story.

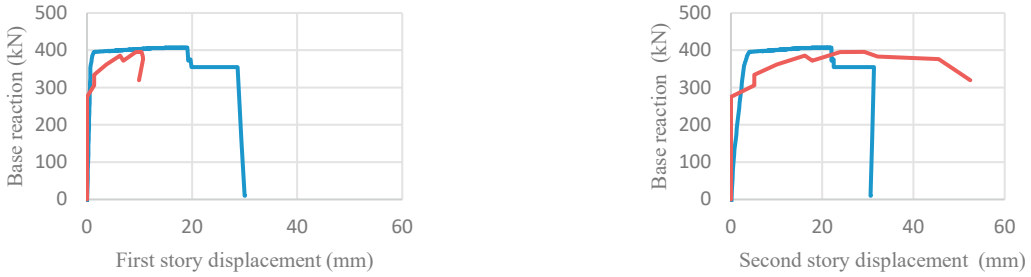

a) first story b) second story

Fig. 5. Force-displacement experimental (red) and numerical (blue) response curve for building 1 at first (a) and second (b) story.

Building 2

Building 2 was analysed in both pre-reinforcement and post-reinforcement conditions. The mechanical properties of the original masonry of building 2 were assumed to be the same as those of building 1 (Table 1).

For the pre-reinforcement condition, the pushover curves of walls A and B are reported in Fig. 6. They are very similar to the corresponding curves of building 1. The plastic hinges at collapse are shown in Fig. 7.

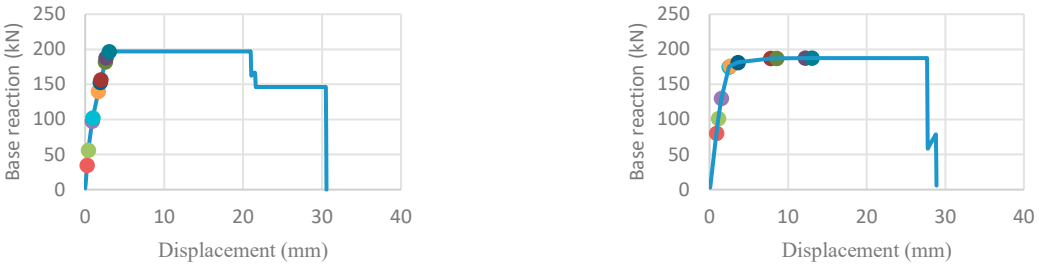

a) wall A b) wall B

Fig. 6. Force-displacement numerical response curves for pre-reinforcement building 2: colored circles correspond to the hinges depicted in Fig. 7.

a) wall A b) wall B

Fig. 7. Plastic hinge distribution at collapse for pre-reinforcement building 2: colored symbols indicate hinges corresponding to the circles depicted in Fig. 6 (circle: flexural hinge, parallelogram: shear link).

The reinforcement of building 2, consisting of a GFRP mesh, was applied on both faces of the masonry on the first story, only on the outer face on the second story. The mechanical characteristics of the reinforced masonry are reported in Table 2.

Table 2. Mechanical properties of reinforced masonry (building 2).

	f (MPa)	f_{v0} (MPa)	τ_0 (MPa)	f_h (MPa)	E (MPa)	G (MPa)
First story	5.460	0.384	0.193	2.730	3800	1500
Second story	5.005	0.245	0.123	2.502	2453	981

The pushover curves of walls A and B in the post-reinforcement conditions are reported in Fig. 8, where the curves in the pre-reinforcement conditions are reported as well for comparison. It can be noted that the reinforcement leads to a doubling of the capacity, in terms of both strength and displacement capacity. For wall A it can be observed that the initial displacement of the plastic branch, and the displacement for which a first decrease of the force occurs, are approximately coincident with those of the non-reinforced wall. For wall B it is possible to notice the presence of a hardening branch before the plastic branch. The plastic hinges at collapse are shown in Fig. 9.

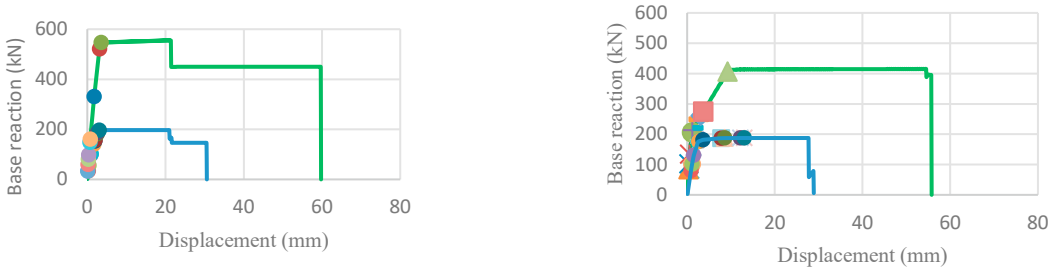

a) wall A b) wall B

Fig. 8. Force-displacement numerical response curves for pre- (blue lines) and post-reinforcement (green lines) building 2: colored circles correspond to the hinges depicted in Fig. 9.

a) wall A b) wall B

Fig. 9. Plastic hinge distribution at collapse for post-reinforcement building 2: colored symbols indicate hinges corresponding to the circles depicted in Fig. 8 (circle: flexural hinge, parallelogram: shear link).

The numerical pushover curves are compared with the experimental ones in Fig. 10. It can be observed that the numerical curves underestimate the strength by about 10%. Differences can also be noted in the type of mechanism: while the numerical analysis envisages a mechanism at the first story, the test shows the activation of a mechanism that affects both the first story and the second story. Accordingly, the displacement capacity is well reproduced for the first story and underestimated by about 40% for the second story.

5. Conclusions

The numerical simulation of the pushover test performed on the Castel di Lama building is studied by means of an equivalent frame model using a force-based formulation for pier and spandrel macroelements.

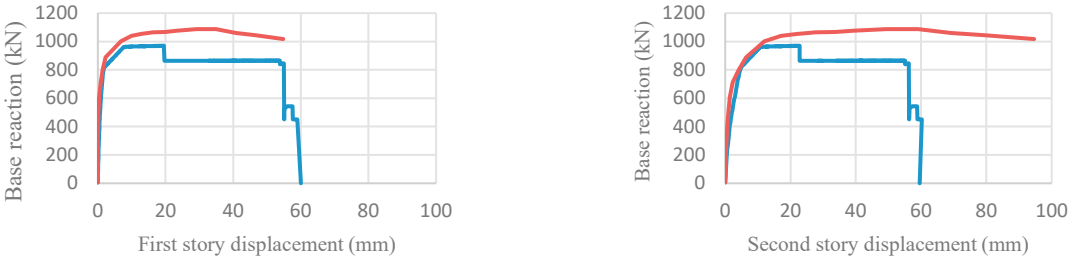

a) first story b) second story

Fig. 10. Force-displacement experimental (red) and numerical (blue) response curve for post-reinforcement building 2 at first (a) and second (b) story.

For the unreinforced masonry (building 1), the resulting pushover curves are in good agreement with the test in terms of strength. As regards the collapse mechanism, the model envisages the failure of the first story, whereas the test activated the failure of the second story. Accordingly, the ultimate displacements are overestimated at the first story and underestimated at the second story. Regarding the reinforced masonry (building 2), the strength is underestimated by about 10%, depending on the mechanical properties adopted for masonry. The ultimate displacements are well reproduced at the first story and underestimated at the second story. The numerical model envisages the failure of the first story, whereas the experimental mechanism involved both the first and the second story.

Future developments will concern the application of a macromechanical nonlocal damage-plastic model reproducing the onset and evolution of degrading mechanisms in masonry, regarded as an equivalent homogenized continuum.

Acknowledgements

The authors are grateful to Yuki Andrea Manieri for the pushover analyses through the equivalent frame model.

References

Addessi, D., Liberatore, D., Masiani, R., 2015. Force-based beam finite element (FE) for the pushover analysis of masonry buildings. International Journal of Architectural Heritage 9(3), 231-243.

Boccamazzo A. et al., 2022. Push ‘o ver: a pushover test program on an existing brickwork construction. Proc. XIX ANIDIS, 11-15 Sept 2022, Turin.

Dolce, M., 1991. Schematizzazione e modellazione degli edifici in muratura soggetti ad azioni sismiche [Modeling of masonry buildings under seismic actions]. L’Industria delle Costruzioni 25(242), 44-57.

Dudine et al., 2022. Push ‘o ver: in situ pushover tests on a bare and a strengthened existing brickwork construction. Proc. XIX ANIDIS, 11-15 Sept 2022, Turin.

Gatta, C., Addessi, D., Vestroni, F., 2018. Static and dynamic nonlinear response of masonry walls. International Journal of Solids and Structures 155, 291-303.

Liberatore, D., Addessi, D., 2015. Strength domains and return algorithm for the lumped plasticity equivalent frame model of masonry structures. Engineering Structures 91, 167-181.

Peruch, M., Spacone, E., Camata, G., 2019. Nonlinear analysis of masonry structures using fiber-section line elements. Earthquake Engineering and Structural Dynamics 48(12), 1345-1364.

Raka, E., Spacone, E., Sepe, V., Camata, G., 2015. Advanced frame element for seismic analysis of masonry structures: model formulation and validation. Earthquake Engineering and Structural Dynamics 44(14), 2489-2506.

Sangirardi, M., Liberatore, D., Addessi, D., 2019. Equivalent frame modelling of masonry walls based on plasticity and damage. International Journal of Architectural Heritage 13(7), 1098-1109.

Siano, R., Roca, P., Camata, G., Pelà, L., Sepe, V., Spacone, E., Petracca, M., 2018. Numerical investigation of non-linear equivalent-frame models for regular masonry walls. Engineering Structures 173, 512-529.